A Novel Coil Structure for Metal Sheet Magnetic Pulse Welding

X. Jiang[1], H. Yu[1,2,3*], H. Li[1], J. Deng[4]

[1] School of Materials Science and Engineering, Harbin Institute of Technology, Harbin, 150001, China
[2] National Key Laboratory for Precision Hot Processing of Metals, Harbin Institute of Technology, Harbin, 150001, China
[3] Suzhou Research Institute, Harbin Institute of Technology, Suzhou, 215104, China
[4] School of Mechanical Engineering and Automation, Fuzhou University, Fuzhou, 350116, China
*Corresponding author. Email: haipingy@hit.edu.cn

Abstract

Magnetic pulse welding (MPW) of metal sheets is an efficient and environment-friendly room temperature solid-state welding technology. However, the process involves significant energy dissipation. Limited by the current coil structure, high energy is required to achieve metallurgical welding of metal sheets. To address this issue, novel coil principle and structure has been proposed. The current is simultaneously concentrated into a section of conductor by a unique circuit design, achieving current summation and amplification, thereby enhancing energy efficiency. Numerical simulations were performed to explore the effects of coil parameters on current density, Lorentz force, and flyer sheet motion, revealing that the coil structure can amplify current by 1.5 to 5.3 times as coil turns increase from 2 to 7. The flyer sheet velocity exceeded the critical welding velocity. Experimental results show successful welding of 1060 (1.0 mm) / DP450 (1.0 mm) at 6.05 kJ and 5754 (1.0 mm) / DP600 (1.0 mm) at 9.8 kJ, with all interfaces displaying metallurgical characteristics. These findings confirm the excellent welding capability of the novel coil at low energy, which results from a significant current amplification effect. This reduces the stringent requirements for magnetic pulse discharge equipment, thereby facilitating the further industrial application of MPW technology.

Keywords

Magnetic pulse welding, Novel coil structure, Metal sheet

1 Introduction

Magnetic pulse welding (MWP) is an environmentally friendly and efficient room-temperature solid-state welding technology. It relies on the electromagnetic force to induce high-speed deformation and collision of the metal plates to be welded, thereby achieving the welding of dissimilar metals. Compared to traditional fusion welding, the advantages of MPW include: a higher tolerance for the differences in physical and chemical properties between dissimilar metals, and a welded interface with no heat-affected zone and minimal intermetallic compounds, among other defects (Kapil and Sharma, 2015).The MWP process for dissimilar metal plates is closely related to the matching of the inherent parameters of the magnetic pulse discharge equipment (such as low inductance, low resistance, and appropriate capacitance) and the coil tooling. However, the development of magnetic pulse discharge equipment involves high-voltage electrical systems, pulse power technology, and other advanced challenges (Liao et al., 2020; Liu et al., 2024). Therefore, to further promote the application of MWP technology in industrial settings, it is essential to conduct fundamental research on novel coil tooling structures.

Traditional E-shaped (Liu et al., 2022) and H-shaped (Li et al., 2021) coils have limitations in terms of low bonding capacity, short service life, and insufficient energy utilization, which restrict the further industrial application of MPW. Zhang et al. (Zhang et al., 2019) found that when the gap between the return arm and the work arm of the traditional E-shaped coil is approximately three times the width of the work arm, the reverse magnetic field generated by the return arm has the least effect on the deformation behavior of the workpiece. To enhance coil efficiency and bonding capacity, Khalil C et al. (Khalil et al., 2020) proposed the O-shaped coil, which exhibits a lower inductance level and allows for the production of higher-quality joints under the same discharge energy. However, much of the current research still focuses on improving traditional coil structures. The method of current flow remains largely unchanged, with large pulse currents still directly passed through a conductor, resulting in significant energy losses.

Therefore, the novel MPW coil principle proposed in this study no longer adheres to the limitations of the flat coil structure. Based on the unique configuration of a coaxial cable, the sinusoidal decaying oscillating discharge current flows through multiple paths nearly simultaneously in the current convergence part, resulting in the superposition and amplification of current intensity (amplitude). This reduces energy losses and improves energy utilization. The effects of the positioning of the coil convergence part and related structural parameters on welding performance were investigated by numerical simulations combined with experiments, ultimately achieving high-quality weld joints.

2 Coil structure and principle

The principle of the novel coil structure for sheet metal magnetic pulse welding proposed in this study is shown in **Fig. 1(a)**. Through circuit design, the energy from the multi-turn coil is concentrated into a section of conductor, thereby improving energy utilization efficiency.

To achieve this concept, as shown in **Fig. 1(b)**, a multi-turn ring circuit is designed, and the converging conductor section is connected in series with each of the ring circuits. This design ensures that the current in each turn of the ring circuit not only flows through each other but also enables superposition and amplification within the converging conductor section. Coaxial cables, with their inherent concentric conductor arrangement, are the optimal material choice to realize this design, as depicted in the schematic diagram in **Fig. 1(c)**. Two different types of novel coil structures have been designed, as shown in **Figs. 1(d) and (e)**, with the converging section placed at either the center or the side of the coil. The current first enters the core wire section of the coaxial cable and directly flows to the current transfer block at the end of the coil. The current is then transferred to the braided wire of the coaxial cable. Since each turn of the braided wire is connected in series with the converging conductor section, the current in each turn of the braided wire flows through the converging conductor section, thereby achieving current superposition and amplification. It is worth noting that due to the instantaneous nature of the current, the current in the converging section is almost simultaneously superimposed, avoiding any situation where the current flows through the converging section at different times.

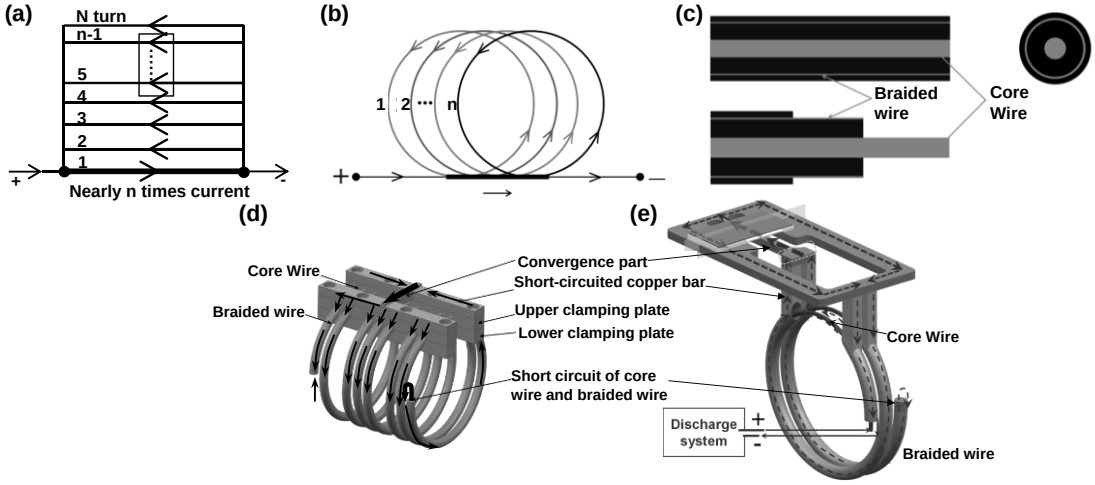

Figure 1: *Schematic diagram of: (a) new coil principle, (b) coil structure, (c) coaxial cable; 3D model of (d) MP coil, and (e) SP coil*

3 Experiment and numerical simulation

3.1 Material selection and equipment

In this study, the materials selected for investigating the welding capability of a novel coil structure include 1060 pure aluminum (thickness: 1 mm), 5754 aluminum alloy (thickness: 0.5 mm and 1 mm), DP450 steel (thickness: 1 mm), and DP600 steel (thickness: 1 mm). All materials have dimensions of 40 × 80 mm. Cu-OFHC was selected as the structural material for the coil, except for the coaxial cable. The material properties of all the selected materials are summarized in **Table 1**.

Material	Yield strength (MPa)	Tensile strength (MPa)	Elongation (%)
1060	31	67	54
5754	90	214	35
DP450	324	445	27
DP600	360	678	26.6
Cu-OFHC	149	261	16

Table 1: *Properties of materials by tensile testing used in this study*

The magnetic pulse discharge equipment used in this study is the self-developed EM20/20 and EM50/18 from Harbin Institute of Technology, which has a 100 μF capacitor and a maximum discharge energy of 20 kJ. EM20/20 and EM50/18 equipment has been successfully applied in industrial production and has high practical application reliability. Various discharge energies were used to study the coil performance, with a collision gap between flying sheet and base sheet set at 2 mm.

3.2 Numerical simulation

In this study, a multi-field coupling numerical simulation of the electromagnetic field, structural field, and force field during MPW overrun was conducted using ANSYS/LS-DYNA software. The meshing methods of MP and SP coils are shown in **Fig. 2**. The coil structure parameters used in this study are listed in **Table 2.** Due to the relatively low inductance of the 4-turn MP coil, it can be paired with EM50/18 that has a higher capacitance (equipment with higher inductance) to achieve optimal performance. In contrast, the 7-turn MP coil, with its higher inductance, is more suitable for EM20/20 with lower capacitance (equipment with lower inductance). Therefore, the MP coil was studied using both types of equipment. For the SP coil, due to the extensive research on its process parameters, only one type of equipment was used for the study. Considering the high strain rates of flyer sheets involved in MPW, the material models for the flyer sheet is based on a simplified Johnson-Cook constitutive model (**Eq. 1**). The parameters for the simplified Johnson-Cook constitutive model of each material are given in **Table 3** (Li et al., 2022; Johnson et al., 1983; Khalil et al., 2021;).

$$\sigma = (A + B\varepsilon^{n}) \cdot \left(1 + C\, ln\frac{\dot{\varepsilon}}{\dot{\varepsilon}_0}\right) \quad (1)$$

Among them, $(A + B\varepsilon^{n})$ represents strain strengthening, and $\left(1 + C\, ln\frac{\dot{\varepsilon}}{\dot{\varepsilon}_0}\right)$ represents strain rate strengthening.

Coil	Turn	Diameter	Pitch
MP	4-EM50/18 and 7-EM20/20	-	-
SP	2-7	150-250	15-45

Table 2: *The coil structure parameters studied in this study*

Material	A	B	n	c
1060	35.5	68.7	0.14	0.015
5754	93.3	166.8	0.28	0.0281
Cu-OFHC	90	292	0.31	0.025

Table 3: *The J-C model parameters of the materials used in this study*

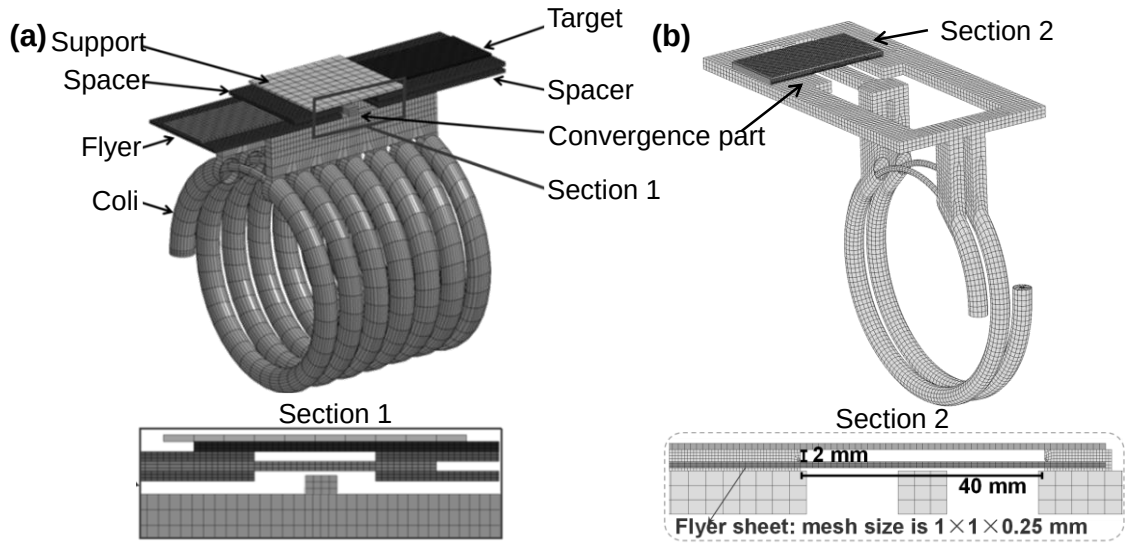

Figure 2: *Grid division results of coils: (a) MP, (b) SP.*

4 Results

4.1 Numerical simulation results

The numerical simulation results of MP coil were analyzed first. The discharge current curve of 7 turns MP coil is shown in **Fig. 3(a)**. The peak current at the coaxial cable part reaches 69 kA when the discharge voltage is 9 kV (4.05 kJ), while the peak current increases to 368 kA at the convergence part, achieving a 5.3-times amplification. The 1/4 discharge current period is 20.5 μs. Within such a short period, the first current peak is reached, which imparts a very high velocity to the flyer sheet. The velocity curves of the flyer sheet under different discharge voltages were obtained, as shown in **Fig. 3(b)**. It can be observed that the collision speed of the flyer sheet is proportional to the discharge voltage (9-12 kV). At a discharge voltage of 12 kV, the maximum collision velocity of the flyer sheet reaches 265 m/s. To investigate the effect of the number of turns on the MP coil, the discharge current of the 4-turn MP coil and the speed imparted to the flyer at different voltages are shown in **Fig. 4**. From the figure, it can be observed that, at higher energy levels, the current in the convergence section of the 4-turn MP coil remains lower than that of the 7-turn MP coil. Additionally, at lower discharge energies, the 7-turn MP coil imparts a higher speed to the flyer. The higher inductance of coils with more turns is disadvantageous for welding. Therefore, further studies on coils with more turns were not conducted.

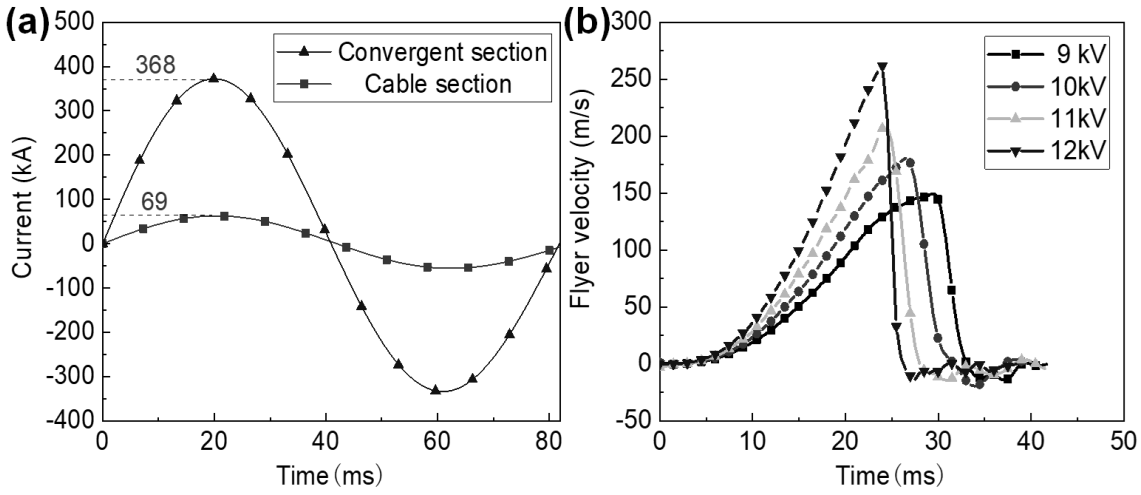

Figure 3: 7 turns MP coil *(a) Current curve at 4.05 kJ, and (b) collision speeds of flying sheet at 9-12 kV*

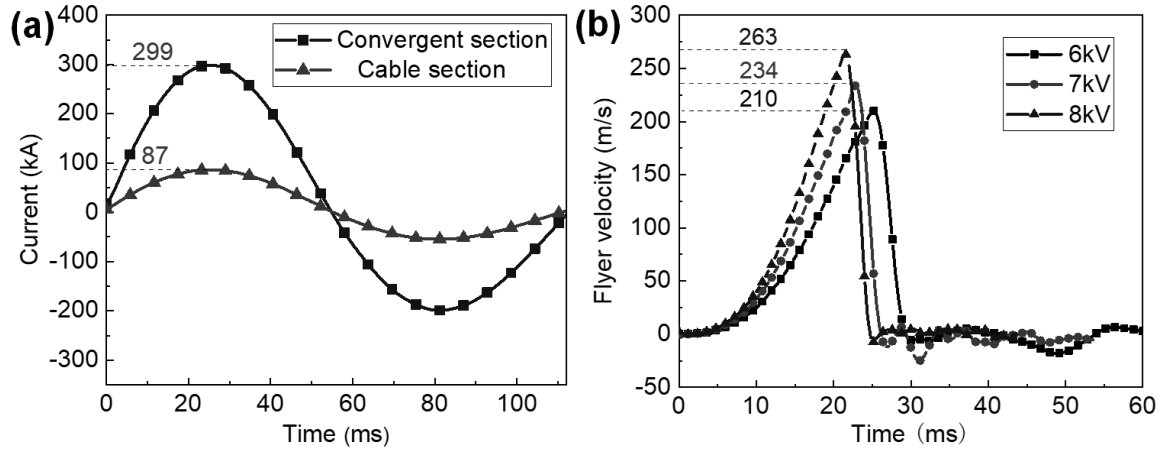

Figure 4: 4 turns MP coil *(a) Current curve at 5.04 kJ, and (b) collision speeds of flying sheet at 6-8 kV*

Due to the different positions of the convergence part, both the inductance and the current distribution vary. More importantly, compared to the coil structure placed within the convergence part, the SP coil allows for the welding of a wider range of plate sizes, as illustrated in the coil structure diagrams in **Figs. 1(d) and (e)**. Therefore, simulations were conducted to evaluate the discharge current and the collision velocity of the flyer sheets for SP coils with different turns, diameters, and pitches. **Fig. 5** presents the discharge current and the collision velocity of the flyer sheet for different SP coil parameters. **Fig. 5(a)** shows the discharge current with varying turns, under a discharge energy of 9.8 kJ. As turns increases from 2 to 7, the current in the coaxial cable part decreases from 126 kA to 67 kA. This reduction in current is primarily due to the increased resistance and inductance resulting from the longer length of the coaxial cable. The current in the convergence part reaches its peak at 270 kA with 6 turns, while the current in the coaxial cable part is only 74.5 kA, with a discharge current period of 108.8 μs. However, this current begins to decrease when the number of turns reaches 7, due to the increase in coil inductance and resistance. As shown

in **Fig. 5(a)**, further increases in the number of turns have little effect on the current amplification. The main reason is that an increase in the number of turns leads to a rise in both resistance and inductance, which in turn causes a decrease in the base current in the coaxial cable. Consequently, a higher amplification factor is unable to drive the current in the convergence section beyond the current level achieved with a lower number of turns. **Fig. 5(b)** shows the flyer sheet velocity, where the 4-turn coil yields the highest velocity. The main reason is that the peak current for the 4-turn SP coil (255 kA in the convergence part and 94 kA in the coaxial cable part) is slightly lower than that of the 6-turn coil, but the discharge current period is shorter. As a result, the flyer sheet experiences higher acceleration over the same collision distance, achieving a higher collision velocity.

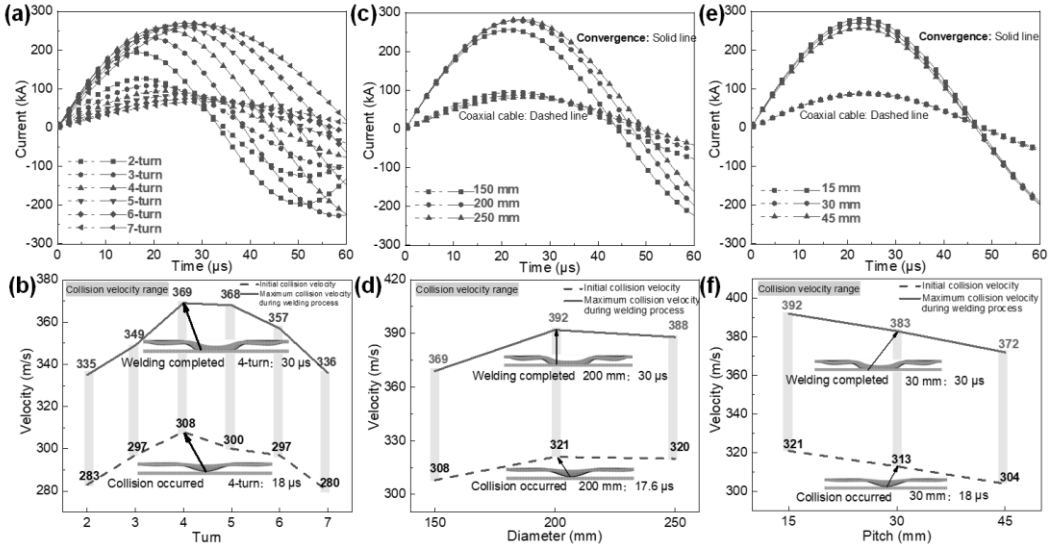

Figure 5*: (a)-(c) The current curves of coils with different turns, diameters, and pitches at 9.8 kJ, (d)-(f) corresponding flying sheet speed*

To further investigate the effect of coil diameter on discharge current for the 4-turn SP coil, **Fig. 5(c)** presents the results. The discharge current is found to be highest when the coil diameter reaches 200 mm. Considering both the flyer sheet velocity and the production flexibility, coils with a diameter of 250 mm are excluded from further investigation due to their large size and relatively low sheet velocity. Further research was conducted on the 4-turn SP coil with a 200 mm diameter, as shown in **Figs. 5(e) and (f)**. As the pitch increases, the coil current gradually decreases. When the pitch is 30 mm, the peak current of the coil is 270 kA (87 kA in the coaxial cable part), achieving a current amplification of 3.1 times. The flyer sheet velocity reaches a maximum of 383 m/s, which is sufficient for achieving the required collision velocity for sheet welding. Based on the overall considerations, a 4-turn SP coil with a 200 mm diameter and a 30 mm pitch is selected for production.

As shown in the **Fig. 6**, compared to the MP coil, the convergence section of the SP coil experiences a smaller Lorentz force at higher energy because it does not interact with the exposed core section of the coaxial cable. This indicates that the SP coil can withstand higher discharge energy without failure, while the convergence section of the MP coil is more prone to deformation and failure. Furthermore, the coaxial cable section of the SP coil, due to its concentric structure of the braided and core wires, results in a cancellation of the

Lorentz force. Additionally, the exposed core section of the coaxial cable is reinforced with epoxy resin in actual production, which extends the coil's lifespan. Therefore, the SP coil is stronger than the MP coil.

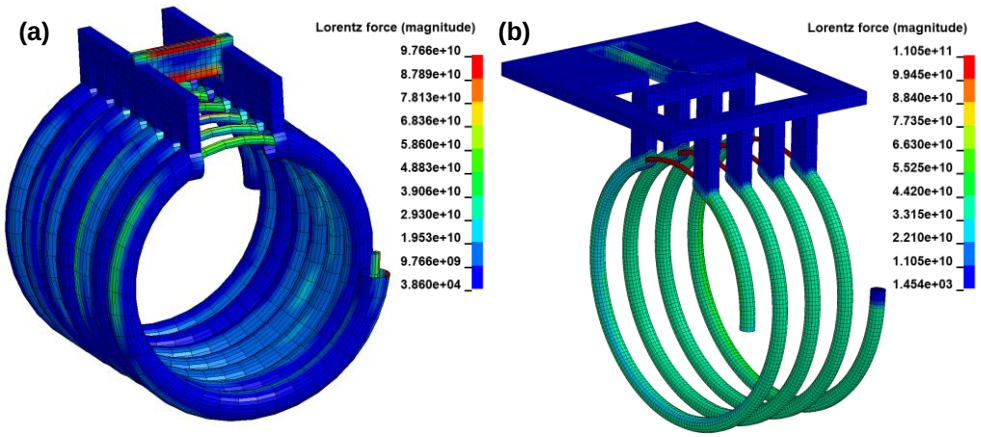

***Figure 6**: Lorentz force distribution map of (a)MP coil at 4.05 kJ, (b) SP coil at 9.8 kJ*

4.2 Experiments

In **Fig. 7(a)**, it can be seen that the width of the flyer sheet is constrained by the length of the coil convergence part of the MP coil. Compared to the SP coil shown in **Fig. 7(b)**, although the MP coil has a higher current amplification factor, the SP coil is not limited by the size of the sheet metal processing. **Figs. 7(d)** and **(e)** show the actual current waveforms measured by the Rogowski coil for the both coil tools. The actual current amplification factor and cycle are similar to the simulation results, thereby confirming the reliability of the simulations results. The welded joints were observed for microstructural at the interface, as shown in **Figs. 8(a) and (d)**. All joints displayed a waveform interface, and Energy Dispersive Spectroscopy (EDS) analysis revealed significant elemental diffusion, confirming the ability of both types of coils to achieve dissimilar metal metallurgical welding.

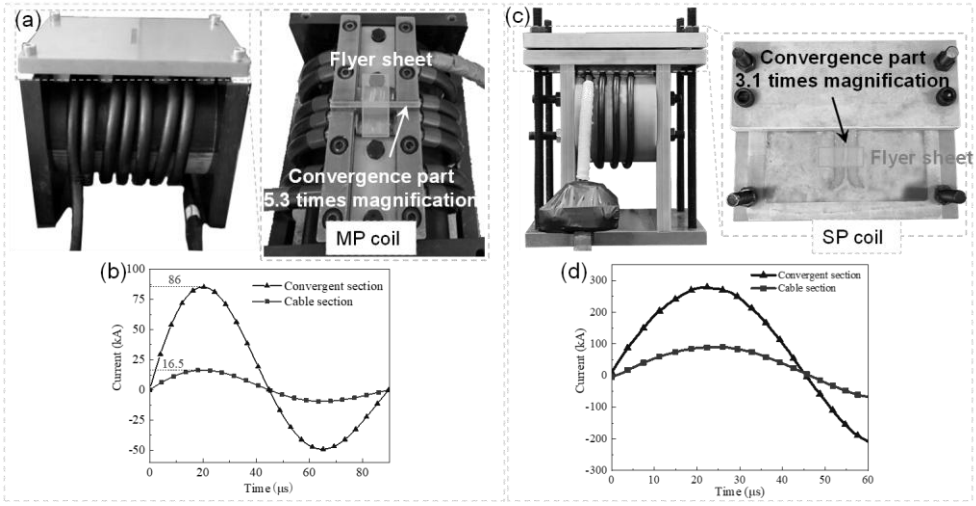

***Figure 7**: (a) MP coil tools, (b) measured current by the Rogowski coil at 2 kV, (c) SP coil tools, (d) measured current by the Rogowski coil at 14 kV*

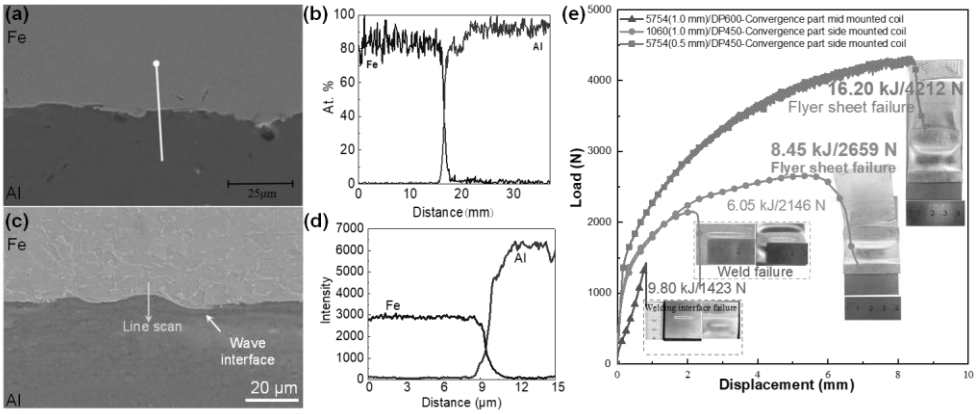

***Figure 8:** Microstructure and EDA line scan of weld interface based on MP and SP coil at 9.8 kJ: (a) and (b): 5754 (1.0 mm)/DP600, (c) and (d): 1060 (1.0 mm)/DP450; (e) Mechanical properties of joints*

Fig. 8(e) presents the mechanical properties of the welded joints. It can be seen that the MP coil achieved a metallurgical weld between 1mm 5754 and DP600 at 9.80 kJ, and the joint's tensile load was 1423 N. Due to the interaction of magnetic fields between the convergence part and the coaxial cable of MP coil, as shown in **Fig1. (d)**, excessive discharge energy can cause deformation and failure of the convergence part. As a result, higher-energy welding experiments cannot be conducted. In contrast, the SP coil allows for a variety of experiments. From the **Fig. 8(e)**, it is evident that high-quality joints can be achieved at higher energy levels. At 8.45 kJ, the 1060 (1.0 mm) / DP450 joint and the 5754 (0.5 mm) / DP450 joint all fractured on the aluminum side. These results confirm the usability of the coil structure and its potential for further development.

5 Conclusions

- A novel coil principle and structure are proposed, utilizing the unique electrical structure of coaxial cable in combination with current circuit control to achieve current accumulation and amplification in the convergence part. Additionally, this study introduces both MP and SP coil structures.

- Numerical simulations were employed to analyze the effects of different structural parameters of coil on the current and flyer sheet velocity. The 7-turn MP coil and the 4-turn/200 mm diameter/30 mm pitch SP coil can achieve current amplifications of 5.3 and 3.1 times, respectively.

- Both coil types are capable of achieving metallurgical welding of dissimilar materials. The SP coil, due to its structural design, can withstand greater reverse Lorentz forces, enabling welding of various material combinations across a range of energy levels.

Acknowledgments

The authors gratefully acknowledge the financial support from the National Natural Science Foundation of China (Grant No. 52175304).

References

Johnson, GR., 1983. *A constitutive model and data for metals subjected to large strains, high strain rates and high temperatures*. Proceedings of the 7th international symposium on ballistics. The Hague: Netherlands;

Kapil, A., Sharma, A., 2015. *Magnetic pulse welding: an efficient and environmentally friendly multi-material joining technique.* Journal of Cleaner Production 100, pp. 35-58.

Khalil, C., Marya, S., Racineux, G., 2020. *Magnetic pulse welding and spot welding with improved coil efficiency—Application for dissimilar welding of automotive metal alloys.* Journal of Manufacturing and Materials Processing 4 (3), pp. 69.

Khalil, C., Marya, S., Racineux, G., 2021. *Construction of physical welding windows for magnetic pulse welding of 5754 aluminum with DC04 steel.* Int. J. Mater. Form. 14, 843–854.

Li, C., Du, J., Zhou, Y., Shen, T., Chen, C.G., 2021. *Development of magnetic pulse welding equipment for plates and experimental research on magnesium/aluminum alloy welding.* Transactions of China Electrotechnical Society 36 (10), pp. 2018–2027

Li, Y., Yang, D., Yang, W., Wu, Z., Liu, C., 2022. *Multiphysics numerical simulation of the transient forming mechanism of magnetic pulse welding.* Metals 12 pp. 1149.

Liao, Z., Li, C., Du, J., Zhou, Y., Wang, X., Shi, X., 2020. *Design and experiments of double-switch electromagnetic pulse welding system*. Energy Reports 6, pp. 964-971.

Liu, Q., Wang, S., Li, G., Cui, J., Yu, Y., Jiang, H., 2022. *A sandwich structure realizing the connection of CFRP and Al sheets using magnetic pulse welding.* Composite Structures 295, pp. 115865.

Liu, W., Peng, W., Li, Z., Zhang, H., 2024. *Energy efficiency improvement method of magnetic pulse welding based on auxiliary capacitance.* The International Journal of Advanced Manufacturing Technology 130 (11), pp. 5869-5878.

Zhang, H., Yang, Z., Ren, L., 2019. *Experimental investigation on structure parameters of E-shaped coil in magnetic pulse welding.* Materials and Manufacturing Processes 34 (15), pp. 1701-1709.